Am J Physiol Regulatory Integrative Comp Physiol 283: R533–R542, 2002;
10.1152/ajpregu.00489.2001.

Dynamic baroreflex control of blood pressure: influence of the heart vs. peripheral resistance

HUANG-KU LIU,[1] SARAH-JANE GUILD,[1] JOHN V. RINGWOOD,[2]
CAROLYN J. BARRETT,[1] BRIDGET L. LEONARD,[1] SING-KIONG NGUANG,[1]
MICHAEL A. NAVAKATIKYAN,[1] AND SIMON C. MALPAS[1]
[1]*Departments of Physiology and Electrical and Electronic Engineering, University of Auckland, Auckland, New Zealand; and* [2]*Department of Electronic Engineering, National University of Ireland, Maynooth, Ireland*

Received 14 August 2001; accepted in final form 22 March 2002

Liu, Huang-Ku, Sarah-Jane Guild, John V. Ringwood, Carolyn J. Barrett, Bridget L. Leonard, Sing-Kiong Nguang, Michael A. Navakatikyan, and Simon C. Malpas. Dynamic baroreflex control of blood pressure: influence of the heart vs. peripheral resistance. *Am J Physiol Regulatory Integrative Comp Physiol* 283: R533–R542, 2002; 10.1152/ajpregu.00489.2001.—The aim in the present experiments was to assess the dynamic baroreflex control of blood pressure, to develop an accurate mathematical model that represented this relationship, and to assess the role of dynamic changes in heart rate and stroke volume in giving rise to components of this response. Patterned electrical stimulation [pseudo-random binary sequence (PRBS)] was applied to the aortic depressor nerve (ADN) to produce changes in blood pressure under open-loop conditions in anesthetized rabbits. The stimulus provided constant power over the frequency range 0–0.5 Hz and revealed that the composite systems represented by the central nervous system, sympathetic activity, and vascular resistance responded as a second-order low-pass filter (corner frequency ≈0.047 Hz) with a time delay (1.01 s). The gain between ADN and mean arterial pressure was reasonably constant before the corner frequency and then decreased with increasing frequency of stimulus. Although the heart rate was altered in response to the PRBS stimuli, we found that removal of the heart's ability to contribute to blood pressure variability by vagotomy and β_1-receptor blockade did not significantly alter the frequency response. We conclude that the contribution of the heart to the dynamic regulation of blood pressure is negligible in the rabbit. The consequences of this finding are examined with respect to low-frequency oscillations in blood pressure.

sympathetic nerve activity; modeling; transfer function; vasculature; rabbit

THE ABILITY OF THE ARTERIAL baroreflex pathway to regulate blood pressure under steady-state conditions is well understood (25). However, there is a paucity of information regarding its dynamic ability over the frequency range 0.001–0.5 Hz. This is particularly relevant when trying to understand the mechanisms that give rise to oscillations between 0.1 and 0.4 Hz. Although there is general acceptance that this oscillation seen in humans at 0.1 Hz involves an action of the sympathetic nervous system on the vasculature, it is a matter of debate as to the origin of the oscillation. It has been suggested that the oscillation results either as a by-product of the central generation of sympathetic nerve activity (SNA) (8, 24) or from the time delay between the arterial baroreceptors sensing blood pressure and the subsequent reflex effect on the vasculature (3, 6, 9, 22, 29). Certainly the available evidence suggests that the oscillation requires the presence of each of the components of the baroreflex pathway, with baroreceptor denervation or sympathectomy abolishing the oscillation in blood pressure (7, 16, 19). Clearly, if measurement of the strength of such oscillations is to develop into a clinically useful tool, it is imperative to understand factors from which cardiovascular variability is derived (23).

Although it is clear that SNA to the vasculature plays an important role in producing the changes in blood pressure with activation of baroreceptors, it is unclear as to what role changes in heart rate (HR) and stroke volume play. It has been assumed that the HR variability arising at 0.1 Hz in humans is a consequence of the arterial baroreflex via blood pressure changes (3), but that the HR changes themselves are not active in sustaining the oscillation in blood pressure. Certainly, with regard to the steady-state condition, the evidence indicates that changes in cardiac output account for <10% of the changes in blood pressure as a result of activation of baroreceptors (11). However, more recent research indicates that, in the human, the changes in HR with breathing under some conditions produce changes in blood pressure (28). This raises the possibility that changes in HR governed via sympathetic and parasympathetic nerve activities may play an important role in governing the dynamic changes in blood pressure.

The aim in the present series of experiments was to assess the dynamic baroreflex control of blood pres-

Address for reprint requests and other correspondence: S. C. Malpas, Dept. of Physiology, Univ. of Auckland Medical School, Private Bag 92019, Auckland, New Zealand (E-mail: S.Malpas@auckland.ac.nz).

The costs of publication of this article were defrayed in part by the payment of page charges. The article must therefore be hereby marked "*advertisement*" in accordance with 18 U.S.C. Section 1734 solely to indicate this fact.

sure, to develop an accurate model that represented this relationship, and to assess the role of dynamic changes in HR and stroke volume in giving rise to components of this response. In anesthetized rabbits we applied a patterned electrical stimulation to the aortic depressor nerve (ADN) and measured the ability of blood pressure to respond to input frequencies between 0 to 0.5 Hz.

METHODS

Animal preparation. Experiments were performed on anesthetized New Zealand White rabbits (n = 8, mean weight 3.1 ± 0.2 kg). All procedures were approved by the University of Auckland Animal Ethics Committee. Induction of anesthesia was by intravenous administration of pentobarbital sodium (90–150 mg Nembutal; Virbac Laboratories New Zealand Ltd.) and was immediately followed by endotracheal intubation and artificial respiration at 1 Hz. Anesthesia was maintained throughout the surgery and experiment by pentobarbital sodium infusion (30–50 mg/h). During surgery 154 mM NaCl solution was infused intravenously at a rate of 0.18 $ml \cdot kg^{-1} \cdot min^{-1}$ to replace fluid losses. A heated blanket and infrared light were used throughout the surgery and experiment to maintain body temperature at ~36°C. The right ADN was located in the cervical region between the vagus and the sympathetic trunk using a dissecting microscope, separated free, and sectioned near its junction with the superior laryngeal nerve. The left and right carotid sinus were exposed, and arterial baroreceptors were denervated by cutting all the visible nerves between the internal and external carotid arteries and stripping these vessels. The left ADN was located, separated free, and placed across a pair of hooked stimulating electrodes. Paraffin oil was applied to the nerve throughout the experiment to prevent dehydration. Arterial pressure was measured from a catheter inserted into either the femoral artery or the central ear artery.

Arterial pressure, HR (which was derived from the arterial pressure waveform), and the electrical stimuli applied to the ADN were sampled at 500 Hz using an analog-to-digital data-acquisition card (Lab-PC+, National Instruments). Calibrated signals were continuously displayed on screen and saved at 500 Hz. At the conclusion of the experiment, each animal was killed with an intravenous overdose of pentobarbital sodium (300 mg).

Experimental protocol. Electrical stimulation of the left ADN was produced using purpose-written software in the LabVIEW graphical programming language (National Instruments) coupled to a Lab-PC+ data-acquisition board (National Instruments). Initially, brief periods (30 s) of ADN stimulation at a variety of pulse amplitudes (frequency 20 or 40 Hz; 2-ms pulse width) were used to establish the voltage required to activate all nerve fibers, i.e., to produce the largest reduction in arterial pressure. The stimulation parameters were based on those previously reported to cause oscillations in arterial pressure in anesthetized rats and rabbits (5, 21). Subsequently, after a 5-min control period, the ADN was then stimulated using a pseudo-random binary sequence (PRBS). The PRBS stimulation was composed of a base frequency of 40 Hz (2-ms pulse width) whose amplitude switched between high voltage (determined as described above, generally between 8 and 10 V) and low voltage (0.1 V) (13). Every 1 s, a decision was made to switch or stay at the current voltage. This creates a signal with a relatively flat power spectrum across the frequency range of interest (0–0.5 Hz). The PRBS stimulus was applied to the nerve for a period of 30 min. After the control period of PRBS stimulation, the β_1-adrenergic receptor antagonist atenolol was administered (250 μg/kg iv) and both left and right vagi were sectioned, the PRBS stimulation was then repeated. The dose of atenolol was adjusted where necessary to ensure minimal change in HR during subsequent ADN stimulation.

Data analysis. The 500-Hz sampled data of the PRBS stimulus and arterial blood pressure were low-pass filtered with an eighth-order Chebyshev type I low-pass filter and resampled at a frequency of 2.5 Hz, which ensured coverage of the frequency range of interest (0–0.5 Hz). For better anti-aliasing performance, the 500-Hz data were low-pass filtered and resampled to 50 Hz first and then to 2.5 Hz.

The decimated (low-pass filtered and resampled) 2.5-Hz data were divided into five segments (1,000 points, 400 s) with 50% overlapping to average out the noise in the signal, thus reducing the spectral variance. Hanning windowing was also applied to reduce the spectral leakage before the fast Fourier transform (FFT) was employed to obtain the spectrum of the signal. The respective power spectral density (PSD) was then calculated as the magnitude squared of the spectrum. This PSD gives the measurement of the energy at various frequencies. As expected, the PSD of the PRBS stimulus was fairly flat up to 0.5 Hz and diminished after 0.5 Hz. Because our previous study had identified that the vasculature acts as a low-pass filter to sympathetic nerve activity, with a corner frequency of 0.28 ± 0.2 Hz (13), it was decided to focus on the baroreceptor input with frequencies <0.5 Hz. Additionally, preliminary testing at a range of frequencies up to 1 Hz revealed generally low coherence (<0.5) between ADN stimulation and the blood pressure response >0.5 Hz.

The transfer function, H(f), between the PRBS stimulus and blood pressure was calculated as shown in the equation below

$$H(f) = \frac{E[P_{xy}(f)]}{E[P_{xx}(f)]} \quad (1)$$

where P_{xy} indicates the cross-spectrum between the PRBS stimulus and blood pressure and was calculated as

$$P_{xy} = DFT(y) \cdot conj[DFT(x)], \quad (2)$$

DFT is the discrete Fourier transform, P_{xx} indicates the autospectra or PSD of the PRBS stimulus and was calculated as

$$P_{xx} = DFT(x) \cdot conj[DFT(x)], \quad (3)$$

and E[X] represents the statistically expected value of X (i.e., an ensemble average operation).

This transfer function describes the system's frequency response. The magnitude, H(f) (expressed in dB, 20 $\log_{10}$ of the gain), and phase, $\angle H(f)$ (expressed in radian), of the frequency response were calculated from the transfer function, respectively. The averaged pure time delay (t_D) was calculated as the slope of the phase response between 0.1 and 0.5 Hz by the following equation in a linear regression manner, as

$$t_D = \frac{-\Delta \angle H(f)}{2\pi \Delta f} \quad (4)$$

It is also important to note that because the voltage required to activate all nerve fibers was different across each individual rabbit, it was necessary to normalize the amplitude of all PRBS stimuli to unity before performing FFT. Thus the unbiased transfer function of each individual rabbit could be compared between rabbits.

The magnitude squared coherence, C_{xy}, between the PRBS stimulus and blood pressure was also estimated by using equation

$$C_{xy} = \frac{|E[P_{xy}(f)]|^2}{E[P_{xx}(f)]E[P_{yy}(f)]} \quad (5)$$

where P_{yy} indicates the autospectra or PSD of the blood pressure.

This coherence function is a measure of linear correlation, in the frequency domain, between the PRBS stimulus and blood pressure. An important use of the coherence function is its application as a test of signal-to-noise ratio and linearity in an input-output relationship. It always lies between a value of 0 to 1, and a value of coherence close to 1 usually gives promise of successful identification, as well as indicating the frequency ranges in which the system can be approximated by a linear model (17). The data sets were divided into 10 segments (300 points, 120 s) with 50% overlapping to estimate the coherence between the PRBS stimulus and arterial pressure.

Statistical analysis. Results are presented as means ± SE. A paired *t*-test was used to compare between two groups. The associated *P* values are shown along with the estimated parameters, and differences were considered statistically significant when $P < 0.05$.

RESULTS

Baseline cardiovascular variables. The control baseline levels of MAP and HR, as measured before ADN stimulation, were 70 ± 3 mmHg and 265 ± 13 beats/min, respectively. At the onset of the PRBS stimulation, there was a rapid fall in MAP and HR to 53 ± 3 mmHg and 237 ± 11 beats/min, respectively (Fig. 1). In some animals, mean blood pressure recovered toward control values over the 30 min of stimulation (not shown). However, a close match between the spectrum amplitudes from the first half and the last half of the data confirmed that the amplitude of the dynamic response was maintained. As the PRBS stimulation sequence is composed of a voltage that goes from essentially zero to a supramaximal voltage level, the arterial pressure and HR displayed corresponding increases and decreases, i.e., an increase in voltage was associated with a decrease in arterial pressure and HR. Figure 1 illustrates this variability across the whole 30-min period of stimulation and also the effect of the rapid high to low switching where a distinct time delay could be observed between the onset of the stimulus and the response.

Frequency response of arterial pressure to ADN stimulation. The transfer function and the coherence between the PRBS stimulus and the arterial pressure response for three individual animals under control conditions is shown in Fig. 2. Although individual animals had slightly different results, the general profile was consistent across animals (Fig. 2).

The gain of the magnitude response was fairly constant below ~0.01 Hz, with an average decay of −30 ± 1.2 dB per decade (calculated by linear regression) above this frequency.

From the phase responses, the inverse blood pressure response relative to the PRBS input was confirmed by the initial phase of π rad at the frequency of 0 Hz, i.e., when the stimulus was high the blood pressure went down. The phase response rolled off steeply in the low frequency range from 0 to ≈0.05 Hz then reached a constant decaying slope beyond 0.05 Hz. The constant slope indicated the presence of pure time delay in the system (between stimulus and the blood pressure response).

One difficulty in conducting such linear transfer function analysis is with the conversion to gain in millimeters Hg per volt of stimulation. Such analysis indicates that increasing levels of stimulus will be associated with increasing levels of response and does not take into account that once all the nerves in the

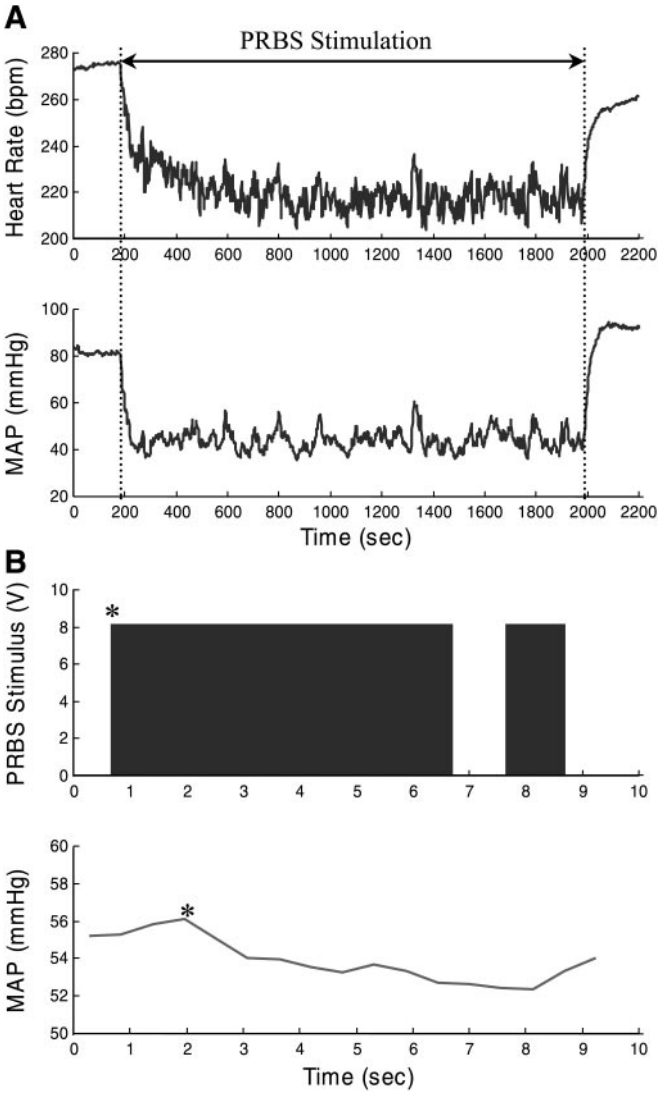

Fig. 1. Effect of a 30-min period of pseudo-random binary sequence (PRBS) stimulation on heart rate and mean arterial pressure (MAP) (*A*). *B*: 10-s period of PRBS and the resultant change in MAP. The PRBS was configured to switch between 0.1 and 8 V. The decision to switch was made every 1 s, which produced an input stimulus containing equal power in the frequency range 0–0.5 Hz. In this example, the PRBS voltage is high for 6 s and produces a decrease in MAP occurring some time after the onset of the stimulus (indicated by *).

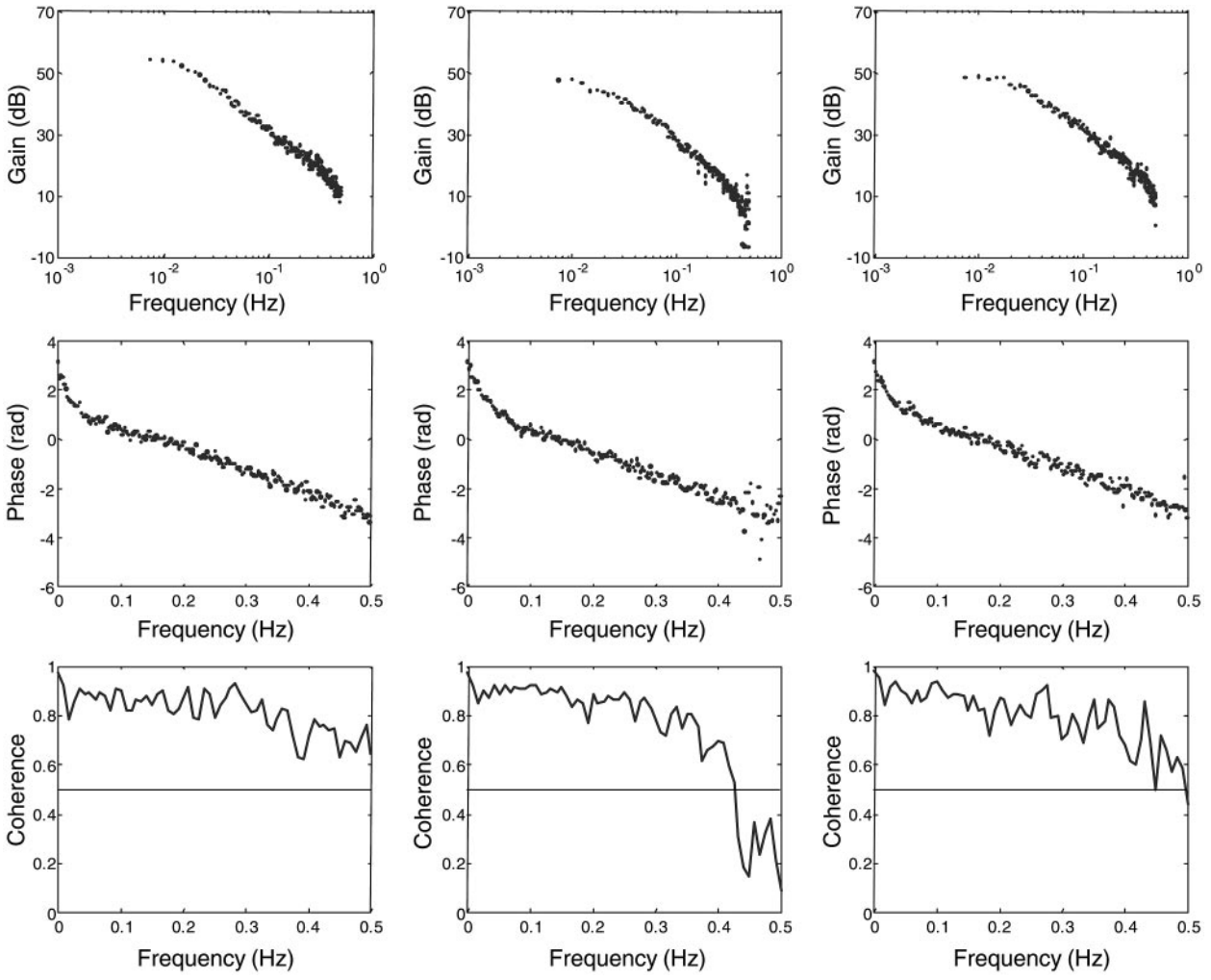

Fig. 2. Transfer functions between PRBS stimulation of the aortic depressor nerve and the blood pressure response for 3 rabbits. Note the high degree of coherence up to 0.5 Hz. The high gain (units mmHg/V in dB) was due to the very low average input power, because our PRBS was composed of 2-ms pulses with a base frequency of 40 Hz, i.e., most of the time the signal was off.

stimulated bundle have been activated there can be no further recruitment of more nerves. It should be noted that a supramaximal voltage was used for the high PRBS voltage. Thus, in reality, although the stimulus intensity may have varied between animals, the input when the stimulus was on was effectively the same for all animals. Hence calculation of the blood pressure spectrum results in a figure that represents the ability of the vasculature to respond to a stimulus where all nerve fibers in the ADN are activated. In reality, because the PRBS stimulus (input) had a fairly flat spectrum, the blood pressure spectrum showed a similar shape to the magnitude response of the transfer function. However, the transfer function parameterization was still crucial for accurate representation of the system phase and gain between the input and output, allowing development of a model to describe the system.

Coherence between the stimulus and response. Under control conditions, the coherence between the PRBS stimulus and arterial pressure response was >0.5 within the frequency range from 0 to 0.5 Hz in most rabbits. The high coherence indicated that changes in arterial pressure were highly linearly dependent on the PRBS stimulus in this frequency range and that the system could be approximated by a linear model (17).

Low-pass filter modeling of the frequency response. Both the magnitude and phase response showed characteristics of a low-pass filter (12). However, it was not clear whether the transfer function should be modeled with a first-order or second-order filter, because the average decay in the magnitude response was 30 ± 1.2 dB per decade and thus halfway between the theoretical 20 dB (first order) and 40 dB (second order). Both models were therefore fitted to the experimental magnitude and phase responses using an optimization-based strategy as given in Guild et al. (13), using a cost function of the form

$$J = \sum_i \{[|G_i| - |\hat{G}_i|]^2 + \rho[\angle G_i - \angle \hat{G}_i]^2\} \qquad (6)$$

where J is the total cost (error) to be minimized, G_i and $\hat{G}_i$ are the measured and modeled frequency response, respectively, and ρ is the phase error weighting relative to the gain error weighting.

This is similar to least squares fitting, but, because the cost function is not linear in the parameters (as required in least squares), an alternative optimization technique is required, such as the Simplex method used here. It was found that, fitting separately to magnitude and phase responses, the root mean squared errors (RMSE) obtained from a second-order low-pass filter were significantly lower than that obtained from a first order (2.28 ± 0.31 vs. 3.80 ± 0.47 dB and 0.19 ± 0.04 vs. 0.26 ± 0.05 rad, 1-tail paired *t*-test, $P < 0.001$ and 0.005, respectively). Therefore, it was concluded the transfer function was more appropriately modeled using a second-order low-pass filter with a constant delay, as given by the following equation

$$G(j\omega) = \frac{K}{(1 - (\omega/\omega_n)^2 + j2\zeta(\omega/\omega_n)} e^{-j\omega t_D} \quad (7)$$

where $G(j\omega)$ represents the frequency response of the system transfer function and the parameters K, ω_n, ζ, and t_D are the gain, natural frequency, damping ratio, and time delay, respectively. The numerical values of the parameters were determined (by numerical search) to give the best agreement between the model's (predicted) output and the measured one. The estimated K, ω_n, ζ, and t_D were 573 ± 118, 0.047 ± 0.01 Hz (equivalent), 2.25 ± 0.26, and 1.01 ± 0.06 s, respectively (Table 1).

Model validation. The best fit curve produced by the second-order low-pass filter model matched closely the observed data in both the magnitude and phase responses in all individual rabbits under control conditions. The RMSE for simultaneously fitted magnitude and phase responses were 2.28 ± 0.31 dB and 0.36 ± 0.09 rad, respectively. Figure 3 shows the magnitude and phase responses predicted by the model from three animals under control conditions. As shown, a close match between the observed and predicted magnitude (in dB) and phase (in rad) was obtained in each rabbit, and the correlation coefficients were 0.974 ± 0.005 and 0.957 ± 0.019, respectively.

To further evaluate the performance of the model, the error of the model in time-domain simulation was investigated for each individual rabbit (same rabbits as used for modeling). The recorded PRBS stimulus was used as the input into the fitted model, with the mismatch between the simulated and recorded arterial pressure representing the error. Figure 4 shows the simulation results from 200 to 400 s from three animals under control conditions. Although the simulated data followed the changes in the arterial pressure correctly, often there was a direct current (DC) offset between the stimulated and observed data. The average RMSE between the simulated and observed arterial pressure was 2.4 ± 0.4 mmHg, although a significant proportion of this is due to the DC offset (e.g., Fig. 4, *middle*).

The coherence between the measured and simulated arterial pressure during PRBS stimulation was used to

Table 1. *Estimated model parameters and the RMSE in magnitude and phase responses under control conditions and with vagotomy and β-blockade*

Rabbit	Gain, mmHg/Stimulus	Damping Ratio	Natural Frequency, Hz	Time Delay, s	Magnitude RMSE, dB	Phase RMSE, rad
			G(jω) (under control condition)			
32	1,198	3.86	0.029	1.07	1.57	0.21
41	275	1.58	0.039	1.03	2.73	0.30
42	852	2.54	0.011	1.31	4.26	0.97
43	486	2.49	0.043	0.99	1.71	0.22
44	457	1.76	0.042	1.01	2.20	0.21
47	149	1.70	0.108	0.92	2.14	0.28
48	468	2.01	0.053	0.76	1.84	0.25
49	700	2.07	0.049	0.95	1.78	0.42
Average	573	2.25	0.047	1.01	2.28	0.36
SD	335	0.74	0.028	0.16	0.88	0.26
SE	118	0.26	0.01	0.06	0.31	0.09
			G(jω) (under the combined treatment of vagotomy and β-blockade)			
32	453	4.49	0.078	1.30	5.26	0.92
41	226	1.30	0.024	1.09	4.49	0.85
42	244	1.01	0.013	1.18	5.98	1.44
43	905	6.08	0.016	1.11	3.99	0.68
44	487	10.00	0.026	1.55	6.93	1.50
47	318	2.19	0.033	0.88	2.96	0.55
48	362	2.44	0.060	0.78	1.91	0.19
49	383	1.26	0.043	0.88	2.80	0.65
Average	422	3.60	0.037	1.09	4.29	0.85
SD	215	3.13	0.022	0.25	1.71	0.44
SE	72	1.04	0.007	0.08	0.57	0.15
Paired *t*-test	0.31(2tailed)	0.27(2tailed)	0.44(2tailed)	0.28(2tailed)	0.004(1tailed)	0.005(1tailed)

$G(j\omega)$, frequency response of the system transfer function; RMSE, root mean squared errors.

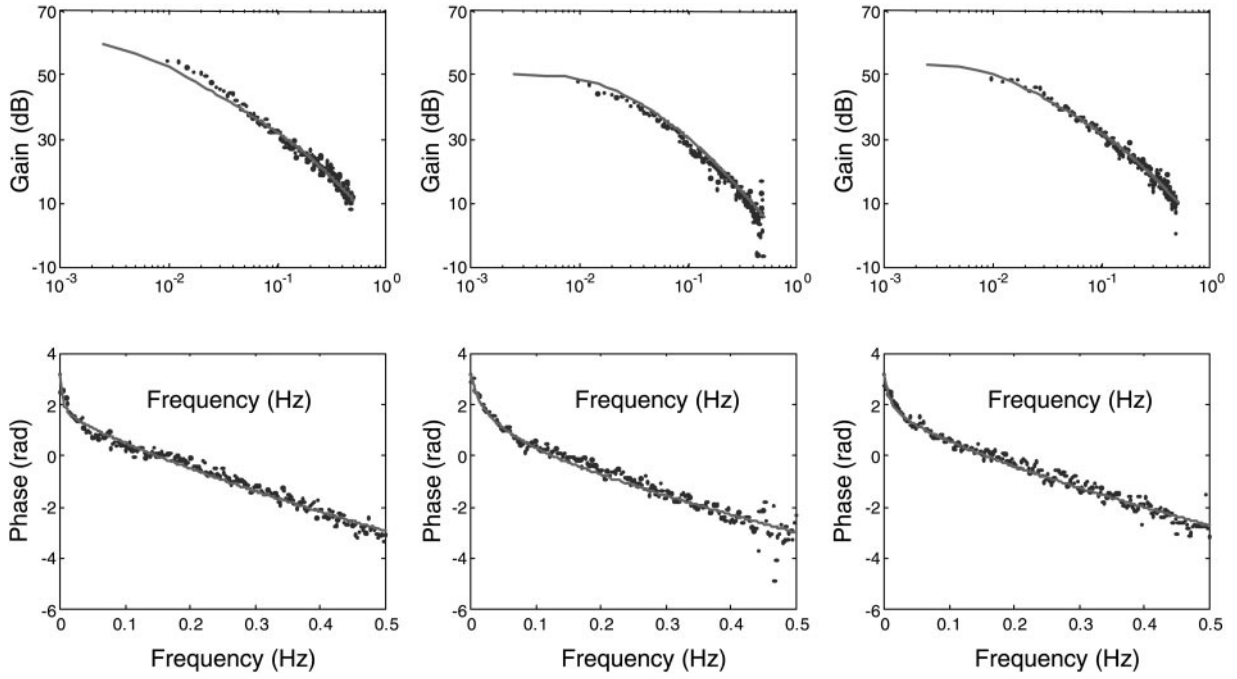

Fig. 3. Actual (dots) and simulated (solid line) magnitude and phase responses under control conditions in 3 rabbits. A close match between the actual and simulated magnitude and phase was obtained in each rabbit.

estimate the validity of the model across the frequency range, where a coherence <0.5 indicates a frequency range not adequately described by the model. The simulated data, based on the model, produced high coherence between 0.01 and 0.5 Hz. Below 0.01 Hz, the coherence fell <0.5, indicating that, at low frequencies, i.e., for slow changes in baroreceptor stimuli (>100 s in period), the model was inaccurate due to a slow recovery in the mean blood pressure level during the stimulus.

Effect of removal of dynamic HR changes on the frequency response of arterial pressure to ADN stimulation. β-Blockade, combined with vagotomy, did not significantly alter resting blood pressure, although it did produce a decrease in heart rate to 206 ± 8 beats/min (from 264 ± 13 beats/min). During the PRBS

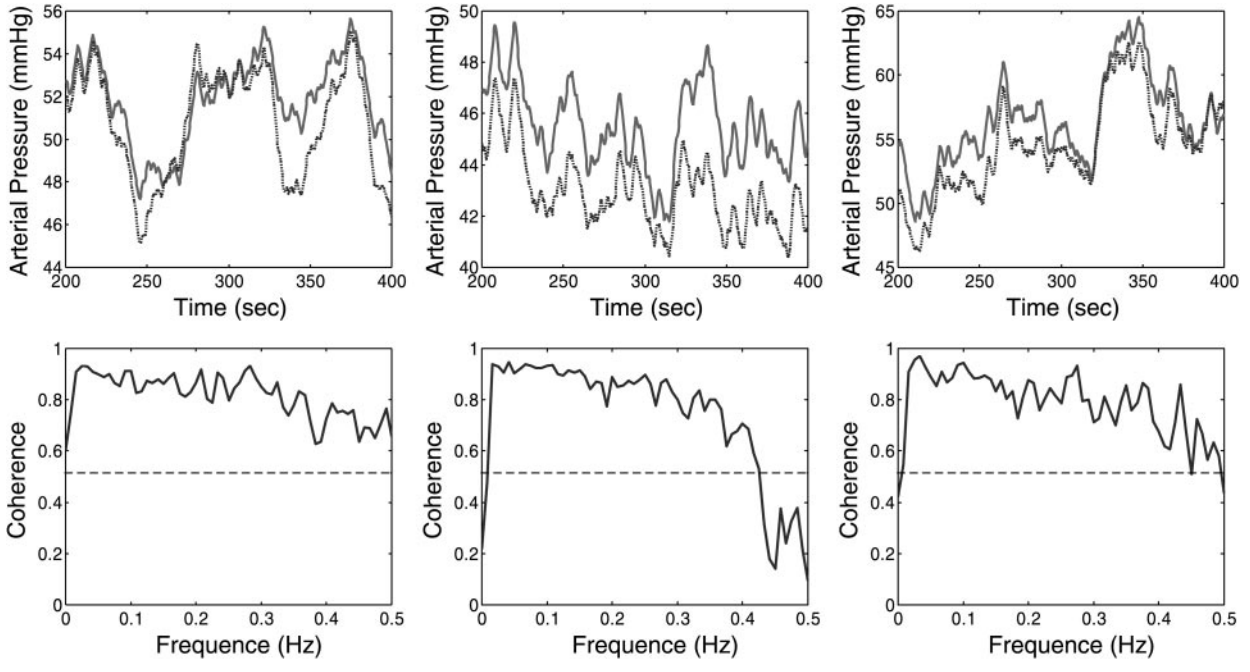

Fig. 4. Actual (dotted) and simulated (solid line) arterial pressure, from 200 to 400 s, in the time-domain under control conditions, and the corresponding coherence between the 2 for 3 rabbits.

stimulation, the decrease in mean blood pressure was not significantly different from that under control conditions (17 ± 4 mmHg); however, the mean HR was unaltered during the PRBS stimulation (calculated from the last 3 min of PRBS stimulation).

All model parameters, namely the gain, damping ratio, natural frequency, and time delay, derived from the second-order low-pass filter model under the combined treatment of vagotomy and β-blockade did not differ significantly from those obtained under control conditions (Table 1). Figure 5 shows the average magnitude and phase responses before and after removal of dynamic HR changes.

The average coherence values between the PRBS stimuli and the resulting blood pressure under control conditions were >0.75 up to ≈0.25 Hz, whereupon it gradually decreased to 0.5 at 0.5 Hz. The average coherence across the whole frequency range for all rabbits was 0.73 ± 0.04. After removal of dynamic HR changes, the coherence was significantly reduced across the whole frequency range (0.50 ± 0.06, $P < 0.0001$) and dropped <0.5 at ≈0.25 Hz (Fig. 5).

In four other animals, neither β-blockade nor vagotomy was performed and PRBS was repeated at 1-h intervals to act as a time control. The frequency responses as described above were unaltered under these conditions.

DISCUSSION

In the present study, patterned (PRBS) electrical stimulation was applied to the ADN to produce changes in blood pressure under open-loop conditions in anesthetized rabbits. The PRBS stimulus provided constant power over the frequency range 0–0.5 Hz and revealed that the composite systems represented by the central nervous system, sympathetic activity and vascular resistance, responded as a second-order low-pass filter with a time delay. The amplitude of variation in arterial pressure was reasonably constant before the corner frequency (≈0.047 Hz) and then decreased with increasing frequency of the stimulus. In other words, the ability of the blood pressure to respond to a stimulus decreased dramatically at high frequencies. Although the HR was reflexly altered in response to the stimuli, we found that removal of the HR (and neurally induced changes in stroke volume) component did not significantly alter the frequency response and thus the ability to control blood pressure in response to baroreceptor stimuli.

Identification of model under open-loop conditions. All experiments were conducted under baroreceptor denervated and thus open-loop conditions. Although this approach previously has been extensively used (5, 14, 15, 20), it is important to identify potential differences between open- and closed-loop conditions with

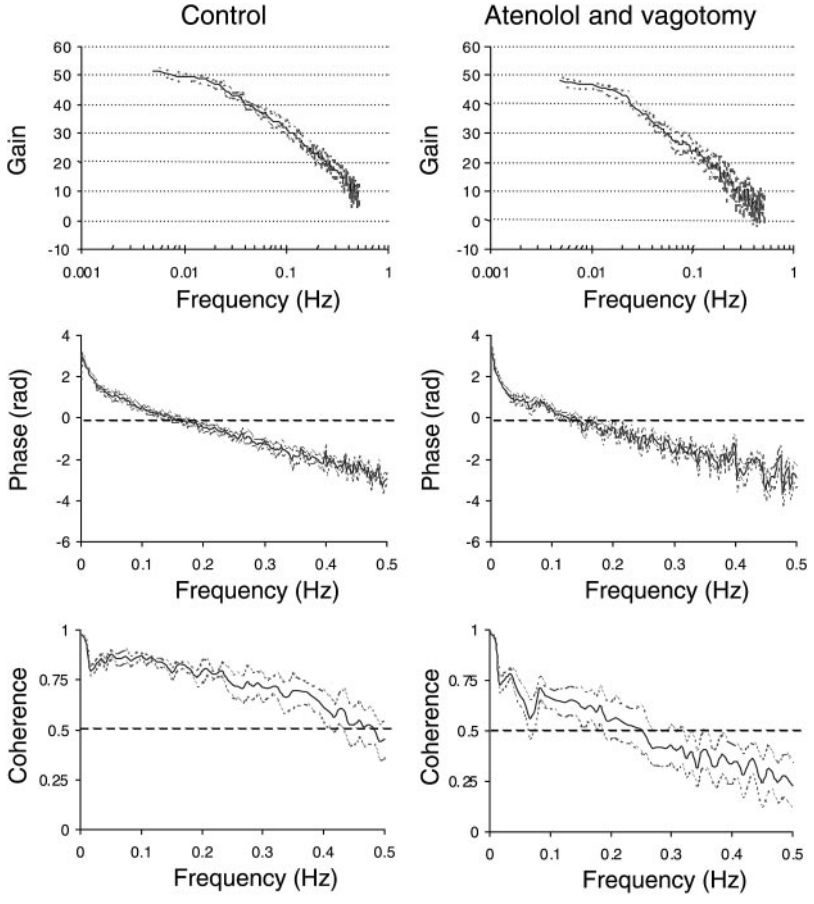

Fig. 5. Averaged magnitude and phase responses and the coherence ($n = 8$) before (*left*) and after removal of dynamic heart rate changes [sympathetic blockade (atenolol) and vagotomy] (*right*). The combined effect of vagotomy and atenolol significantly decreased the coherence between the PRBS stimulus and arterial pressure (0.73 ± 0.04 vs. 0.50 ± 0.06, 1-tail paired *t*-test, $P < 0.0001$). Dotted lines indicate the SE around the mean.

regard to the results we obtained. The rationale for identification under open-loop conditions is that it gives information about each component of the feedback loop, excluding the baroreceptors. Under closed-loop conditions, any variations due to treatment will be diminished due to effects of feedback, given the sensitivity reduction that feedback provides (10).

We applied patterned electrical stimulation of the ADN in a pseudo-random fashion. This allowed us to apply stimulation across a very large frequency range and with equal power, which also allows good frequency resolution. This range of frequencies (0.008–0.5 Hz) is larger than has previously been examined. Although we accept that electrical stimulation of nerves cannot precisely mimic the natural pattern of activation that would be carried within the baroreceptor nerves, it does allow a precise input to the system to be applied, with other potentially conflicting contributions held constant. Although Bertram et al. (4, 5) also employed ADN electrical stimulation in rats, they only excited the system at selected frequencies, and the lowest stimulus frequency was at 0.03 Hz, i.e., the frequency resolution was poor and no information about the system was obtained <0.03 Hz. We previously found that the renal vasculature exhibits resonant-like behavior when the renal nerves were stimulated using PRBS stimuli (13) and we wondered if such resonance would be apparent within the total cardiovascular response. We felt that applying stimulation at set frequency steps as Bertram et al. (5) had done would potentially miss such resonance.

We were able to develop a mathematical model that was able to describe most of the variability in the blood pressure response to baroreceptor stimulation between 0.01 and 0.5 Hz. Because arterial baroreflexes are the principal regulators of short-term control of blood pressure and are known to reset with prolonged steady-state changes in blood pressure, it is important to develop models that are as reflective of the natural condition as possible. Although previous studies measured the dynamic responsiveness to baroreceptor stimulation, there have been few attempts to create and validate a mathematical model of this response. The basis for any developed model lies in experimental observations of such factors as the pure time delay, other phase effects, and gain at different frequencies and these parameters help to quantify variations in comparative studies, such as that undertaken here. Some of the model parameters are easily related to physical quantities. Clearly, the pure delay represents efferent and afferent delays, along with conduction through the central nervous system and any other synaptic connections. The low-pass nature of the model reflects the inertia, or relatively slow response, of smooth muscle, etc., indicating their relatively slow response to high-frequency stimuli. This is quantified through the time constants, or equivalently, the resonant frequency of the system.

It is possible that the gain of the frequency response curve could be different under conscious and closed-loop conditions and this may mean that the response to an input stimulus could be greater than the spectrum amplitudes imply. We suggest that, although the level of the frequency response may shift up and down relative to the level of anesthesia, the shape of the frequency response will not change. Thus, in relative terms, an input at 0.1 Hz will produce a change in blood pressure that is in the same proportion to a response to a 0.2-Hz input, under all conditions. Although our study does not provide direct evidence that the same shape frequency response exists under all conditions, if one considers the factors that are known to determine the frequency response, e.g., the fixed nature of signal transduction at the vasculature, nerve conduction velocity, or central nervous system processing times (18), then it is probable that these components remain stable.

Relative role of the heart in the frequency response of blood pressure. A central aim of the present study was to test for differences in frequency response of the baroreflex control of blood pressure, with and without the influence of cardiac effectors, i.e., baroreflexly induced changes in HR and stroke volume. It is well established that HR contains variability associated with respiration and at 0.1 Hz in humans. Although there is evidence that these oscillations result from the baroreflex feedback pathway, it has also been suggested that the HR can contribute to the variability observed in blood pressure in an independent manner. During atrial pacing, it appears that respiratory-related oscillations in HR can contribute to respiratory oscillations in blood pressure (2, 28). Furthermore, there is evidence that respiratory centers within the central nervous system can directly influence HR independently of changes in blood pressure (1). However, in the present study, we found that the changes in HR due to either vagal or sympathetic activity slightly reduced the gain of the transfer function between PRBS stimulus and arterial pressure but not the general shape of the profile. The small effect of neural regulation of the heart in the blood pressure responsiveness may be explained through the relationship between HR, stroke volume, and the resulting cardiac output, where the increase in HR reduces the heart filling time and thus stroke volume, leading to a disproportionately smaller change in cardiac output than one might expect, given the change in HR. It must be acknowledged that changes in steady-state sympathetic activity to the heart will also lead to increased contractility of the myocardium and higher stroke volume (not measured). However, the changes in cardiac output during baroreceptor stimulation appear to have little effect on the dynamic blood pressure response.

Implications for oscillations in blood pressure. It has been proposed that the slow oscillation in blood pressure results from delayed feedback between arterial baroreceptors and the vasculature, where a change in blood pressure is sensed by arterial baroreceptors and adjusts sympathetic outflow to the vasculature and therefore peripheral resistance, leading to a change in blood pressure in an attempt to buffer the initial change in blood pressure (9). The critical point is the

combination of a series of time delays present between baroreceptors, the central nervous system, sympathetic outflow, and the vasculature's response. This means that the input change in blood pressure results in an output change in vascular resistance that is slightly shifted in time and, instead of buffering the initial change in blood pressure, it leads to the development of its own change in blood pressure.

Inasmuch as we electrically stimulated the baroreceptor nerves directly, our frequency response does not include the response of the baroreceptors themselves. The frequency response of the baroreceptors has been previously studied by altering the carotid sinus pressure with a servo pump in a PRBS fashion instead of using electrical stimulation (14). This group has shown that the transfer function between the pressure perturbation and ADN activity exhibits a phase lead characteristic (27). From their work, it appears that the maximal phase lead is 15 degrees and, given that our model displays second-order plus delay characteristics, the complete model would, therefore, have the capacity to produce sustained oscillations, because a total phase lag of 180 degrees is easily achievable.

In a linear system, the criterion for sustained feedback oscillation is that the open-loop gain must be greater than one (>0 dB) when the open-loop phase crosses the −180 degree line, i.e., a positive feedback condition exists around the baroreflex loop. For a nonlinear system, the criterion for sustained feedback oscillation is that the complex frequency response of the linear component intersects the describing function line corresponding to the nonlinear element (26). Of importance, in either case, is the gain of the system at the frequency when the phase is −180 degrees (calculated to be 0.17 ± 0.015 Hz). Because quantification of the DC gain is likely to be altered with anesthesia and a model for the baroreceptors has not been parameterized (the relationship between arterial pressure and ADN activity), no definitive conclusions regarding the likelihood of feedback oscillations can be made. However, using the results of Sato et al. (27), which indicate a lead-lag characteristic for the baroreceptors, the composite phase plot indicates a crossover frequency of 0.19 Hz, representing a small shift to the crossover frequency. After cardiac denervation, there is a small shift in crossover frequency (again including the phase contribution from the baroreceptors) to 0.16 Hz. The above assumes that the oscillation is due to linear components only, where the critical phase point is −180 degrees. In the case of a nonlinear limit cycle (26), any imaginary components in the describing function could result in a small movement of the critical phase point from −180 degrees. However, it is felt that, in such a case, the difference between the control and denervated cases would be, to a large extent, similar.

Given the relatively insignificant change in the frequency response characteristics between control and the vagotomy/β-blockade condition, in conjunction with the derived relationship between frequency response and feedback oscillations, we therefore conclude that any feedback oscillation is primarily due to feedback around the peripheral resistance loop.

Limitations. We observed that during the PRBS stimulation there was a recovery in the mean blood pressure level toward control values over the 30 min of stimulation in some animals, although the dynamic response was maintained. Although this did not affect the frequency response shape, it was obvious in the time-domain simulation. Because the recovery could not be modeled by a linear second-order low-pass filter, there was a DC offset between the stimulated and observed arterial pressure (Fig. 4, *top*). This indicates that, although our model describes the frequency range between 0.01 and 0.5 Hz (Fig. 4, *bottom*), changes in baroreceptor stimuli longer than 100 s (<0.01 Hz) could not be adequately modeled and may be reflective of other hormonal systems acting over longer time scales.

It should also be noted that the PRBS provided stimulation in only one direction (inhibition) and mimics the response to an increase in blood pressure, i.e., producing increased ADN activity, decreased SNA, and arterial pressure. While the normal situation is one that sees both increases and decreases in baroreceptor activity, it is unlikely that this modifies the shape of the transfer function (which is the important finding of our study). Ikeda et al. (14) identified a similar shape gain and phase to the present study. Thus, although the level of the frequency response may shift up and down relative to the level of anesthesia and the type of stimulus provided (sinusoidal vs. PRBS), the shape of the frequency response is unlikely to be altered.

It is also possible that other nonlinear variables such as resting HR, blood pressure, or level of sympathetic nerve activity are important in the determination of the transfer function parameters. Our approach was based on a linear systems theory, which carries the assumptions of superposition, linear model structures, and frequency response. It is possible that there are some nonlinear effects, which may result in linear model parameters varying at different operating points or between different animals. However, the relatively small standard deviation figures obtained suggest that, in the main, the linearity assumption is vindicated.

In summary, we found that the dynamic frequency response of the baroreflex pathway, comprising the central nervous system, sympathetic activity, and changes in vascular resistance, could be modeled by a second-order low-pass filter with a constant delay. Because the model parameters were not significantly altered by the removal of the influence of the heart, we conclude that the contribution of the heart to the dynamic regulation of blood pressure is negligible in the rabbit. With regard to the prediction of low-frequency oscillations in blood pressure, the potential of the baroreflex to produce oscillations is not significantly altered with the removal of the cardiac branch, although there may be a small downward shift in frequency.

This work was supported by the Marsden Fund of New Zealand.

REFERENCES

1. **AlAni M, Forkins AS, Townend JN, and Coote JH.** Respiratory sinus arrhythmia and central respiratory drive in humans. *Clin Sci (Colch)* 90: 235–241, 1996.
2. **Badra LJ, Cooke WH, Hoag JB, Crossman AA, Kuusela TA, Tahvanainen KUO, and Eckberg DL.** Respiratory modulation of human autonomic rhythms. *Am J Physiol Heart Circ Physiol* 280: H2532–H2674, 2001.
3. **Bernardi L, Leuzzi S, Radaelli A, Passino C, Johnston JA, and Sleight P.** Low-frequency spontaneous fluctuations of R-R interval and blood pressure in conscious humans: a baroreceptor or central phenomenon? *Clin Sci (Colch)* 87: 649–654, 1994.
4. **Bertram D, Barres C, Cheng Y, and Julien C.** Norepinephrine reuptake, baroreflex dynamics, and arterial pressure variability in rats. *Am J Physiol Regul Integr Comp Physiol* 279: R1257–R1267, 2000.
5. **Bertram D, Barres C, Cuisinaud G, and Julien C.** The arterial baroreceptor reflex of the rat exhibits positive feedback properties at the frequency of Mayer waves. *J Physiol* 513: 251–261, 1998.
6. **Burgess DE, Hundley JC, Li SG, Randall DC, and Brown DR.** First-order differential-delay equation for the baroreflex predicts the 0.4-hz blood pressure rhythm in rats. *Am J Physiol Regul Integr Comp Physiol* 273: R1878–R1884, 1997.
7. **Cerutti C, Barres C, and Paultre C.** Baroreflex modulation of blood pressure and heart rate variabilities in rats: assessment by spectral analysis. *Am J Physiol Heart Circ Physiol* 266: H1993–H2000, 1994.
8. **Cooley RL, Montano N, Cogliati C, van de Borne P, Richenbacher W, Oren R, and Somers VK.** Evidence for a central origin of the low-frequency oscillation in RR-interval variability. *Circulation* 98: 556–561, 1998.
9. **DeBoer R, Karemaker J, and Strackee J.** Hemodynamic fluctuations and baroreflex sensitivity in humans: a beat-to-beat model. *Am J Physiol Heart Circ Physiol* 253: H680–H689, 1987.
10. **Dorf RC and Bishop RH.** *Modern Control Systems*. New Jersey: Upper Saddle River, NJ: Prentice Hall, 2001.
11. **Faris IB, Jamieson GG, and Ludbrook J.** The carotid sinus-blood pressure reflex in conscious rabbits: the relative importance of changes in cardiac output and peripheral resistance. *Aust J Exp Biol Med Sci* 59: 335–341, 1981.
12. **Golten J and Verwer A.** *Control System Design and Simulation*. London: The McGraw-Hill Companies, 1997.
13. **Guild SJ, Austin PC, Navakatikyan M, Ringwood JV, and Malpas SC.** Dynamic relationship between sympathetic nerve activity and renal blood flow: a frequency domain approach. *Am J Physiol Regul Integr Comp Physiol* 281: R206–R610, 2001.
14. **Ikeda Y, Kawada T, Sugimachi M, Kawaguchi O, Shishido T, Sato T, Miyano H, Matsuura W, Alexander J, and Sunagawa K.** Neural arc of baroreflex optimizes dynamic pressure regulation in achieving both stability and quickness. *Am J Physiol Heart Circ Physiol* 271: H882–H890, 1996.
15. **Imaizumi T, Harsaswa Y, Ando SI, Sugimachi M, and Takeshita A.** Transfer function analysis from arterial baroreceptor afferent activity to renal nerve activity in rabbit. *Am J Physiol Heart Circ Physiol* 266: H36–H42, 1994.
16. **Jacob HJ, Ramanathan A, Pan SG, Brody MJ, and Myers GA.** Spectral analysis of arterial pressure lability in rats with sinoaortic deafferentation. *Am J Physiol Regul Integr Comp Physiol* 269: R1481–R1488, 1995.
17. **Johansson W.** *System Modeling and Identification*. NJ: Englewood Cliffs: Prentice Hall, 1993.
18. **Julien C, Malpas SC, and Stauss HM.** Sympathetic modulation of blood pressure variability. *J Hypertens* 19: 1707–1712, 2001.
19. **Julien C, Zhang ZQ, Cerutti C, and Barres C.** Hemodynamic analysis of arterial pressure oscillations in conscious rats. *J Auton Nerv Syst* 50: 239–252, 1995.
20. **Kawada T, Ikeda Y, Sugimachi M, Shishido T, Kawaguchi O, Yamazaki T, Alexander J, and Sunagawa K.** Bidirectional augmentation of heart rate regulation by autonomic nervous system in rabbits. *Am J Physiol Heart Circ Physiol* 271: H288–H295, 1996.
21. **Kubo T, Imaizumi T, Harasawa Y, Ando SI, Tagawa T, Endo T, Shiramoto M, and Takeshita A.** Transfer function analysis of central arc of aortic baroreceptor reflex in rabbits. *Am J Physiol Heart Circ Physiol* 270: H1054–H1062, 1996.
22. **Madwed J, Albrecht P, Mark R, and Cohen R.** Low-frequency oscillations in arterial pressure and heart rate: a simple computer model. *Am J Physiol Heart Circ Physiol* 256: H1573–H1579, 1989.
23. **Malpas SC.** Neural influences on cardiovascular variability: possibilities and pitfalls. *Am J Physiol Heart Circ Physiol* 282: H6–H20, 2002.
24. **Montano N, Gnecchi-Ruscone T, Porta A, Lombardi F, Malliani A, and Barman SM.** Presence of vasomotor and respiratory rhythms in the discharge of single medullary neurons involved in the regulation of cardiovascular system. *J Auton Nerv Syst* 57: 116–122, 1996.
25. **Nishida Y, Chen QH, Zhou MS, and Horiuchi J.** Sinoaortic denervation abolishes pressure resetting for daily physical activity in rabbits. *Am J Physiol Regul Integr Comp Physiol* 282: R649–R849, 2002.
26. **Ringwood JV and Malpas SC.** Slow oscillations in blood pressure via a nonlinear feedback model. *Am J Physiol Regul Integr Comp Physiol* 280: R1105–R1115, 2001.
27. **Sato T, Kawada T, Shishido T, Miyano H, Inagaki M, Miyashita H, Sugimachi M, Knuepfer MM, and Sunagawa K.** Dynamic transduction properties of in situ baroreceptors of rabbit aortic depressor nerve. *Am J Physiol Heart Circ Physiol* 274: H358–H365, 1998.
28. **Taylor JA and Eckberg DL.** Fundamental relations between short-term RR interval and arterial pressure oscillations in humans. *Circulation* 93: 1527–1532, 1996.
29. **Wessling KH and Settels JJ.** Baromodulation explains short term blood-pressure variability. In: *Psychophysiology of Cardiovascular Control*, edited by Orlebeke JF, Mulder J, and VanDoornen LJP. New York: Plenum, 1985, p. 69–97.